


Phenylboronic ester-modified polymeric nanoparticles for promoting TRP2 peptide antigen delivery in cancer immunotherapy

Qiyang Wang^{a,b,c,*} , Zhipeng Dong^{a,*}, Fangning Lou^a, Yunxue Yin^a, Jiahao Zhang^a, Hanning Wen^a, Tao Lu^a and Yue Wang^a

^aKey Laboratory of Biomedical Functional Materials, School of Sciences, China Pharmaceutical University, Nanjing, Jiangsu, China; ^bCenter for Cutaneous Biology and Immunology Research, Department of Dermatology, Henry Ford Health System, Detroit, Michigan, USA; ^cImmunology Research program, Henry Ford Cancer Institute, Henry Ford Health System, Detroit, Michigan, USA

ABSTRACT

The tremendous development of peptide-based cancer vaccine has attracted incremental interest as a powerful approach in cancer management, prevention and treatment. As successful as tumor vaccine has been, major challenges associated with achieving efficient immune response against cancer are (1) drainage to and retention in lymph nodes; (2) uptake by dendritic cells (DCs); (3) activation of DCs. In order to overcome these barriers, here we construct PBE-modified TRP2 nanovaccine, which comprises TRP2 peptide tumor antigen and diblock copolymer PEG-b-PAsp grafted with phenylboronic ester (PBE). We confirmed that this TRP2 nanovaccine can be effectively trapped into lymph node, uptake by dendritic cells and induce DC maturation, relying on increased negative charge, ROS response and pH response. Consistently, this vehicle loaded with TRP2 peptide could boost the strongest T cell immune response against melanoma in vivo and potentiate antitumor efficacy both in tumor prevention and tumor treatment without any exogenous adjuvant. Furthermore, the TRP2 nanovaccine can suppress the tumor growth and prolong animal survival time, which may result from its synergistic effect of inhibiting tumor immunosuppression and increasing cytotoxic lymphocyte (CTL) response. Hence this type of PBE-modified nanovaccine would be widely used as a simple, safe and robust platform to deliver other antigen in cancer immunotherapy.

ARTICLE HISTORY

Received 17 April 2022
Revised 25 May 2022
Accepted 30 May 2022

KEYWORDS



PBE; nanovaccine; immunotherapy; polymer


1. Introduction

A well-established aspect of the immune system plays a vital role in cancer treatment and prevention (LiuJiang et al., 2018; Wang et al., 2020; Zhang and Zhang, 2020; Pajjens et al., 2021; Varade et al., 2021). However, the immune system in cancer patients is normally suppressive, therefore it can't be elicited to recognize and subsequently eradicate tumor cells (Sengupta et al., 2010; Mahasa et al., 2016; Merlo et al., 2016; Musetti & Huang, 2018). Tumor vaccines represent one of the successful breakthroughs in cancer immunotherapy, because it can mobilize the hampered immune system and induce long-lasting tumor-specific immune responses (Melerio et al., 2014; Hu et al., 2018; Ugur & Özlem, 2018). In particular, peptide-based vaccines (Wiedermann et al., 2013; Kuai et al., 2017; 2018; Shi et al., 2020) focusing on only a single or a few critical epitopes have the unique potential, due to their safety, specificity and reproducibility. Nevertheless, we know that the monotherapy of peptide tumor antigen without any incorporation hardly has excellent efficacy in cancer immunotherapy clinically.

Accumulating evidences have shown the insufficient immunogenicity of these vaccines peptide-based vaccines usually results in poorly primed cell-mediated immune responses in both clinical and preclinical studies, because of rapid degradation, low affinity and immunological tolerance (Slingluff, 2011; Malonis et al., 2020). To overcome this limitation, high-performance nanomaterials are pursued to construct tumor nanovaccines which help deliver peptide tumor antigen efficiently in cancer immunotherapy (Zhu et al., 2017; Lai et al., 2018; Singha et al., 2018; Martin et al., 2020; Sun et al., 2020; Yang et al., 2020).

Lymph nodes are the important sites for generating antigen-specific immune responses (Zhu et al., 2017; Singha et al., 2018). During the process of vaccination, peptide vaccine can firstly drain into lymph nodes and then be trapped in it for DC uptake. Subsequently DCs will become mature, inducing potent cellular immune response. Many studies show that particles with a suitable size (from 10 to 100 nm) (Irvine et al., 2015; Gause et al., 2017) can be trapped in lymph node for sustaining antigen presenting. Apart from the size, nanovaccine requires a negative surface charge for

CONTACT Yue Wang  zwy_1115@126.com; Tao Lu  lut163@163.com  Key Laboratory of Biomedical Functional Materials, School of Sciences, China Pharmaceutical University, Nanjing, Jiangsu Province, 211198, China
†Qiyang Wang and Zhipeng Dong contributed equally to this work.

 Supplemental data for this article is available online at <https://dx.doi.org/10.1080/10717544.2022.2086941>.

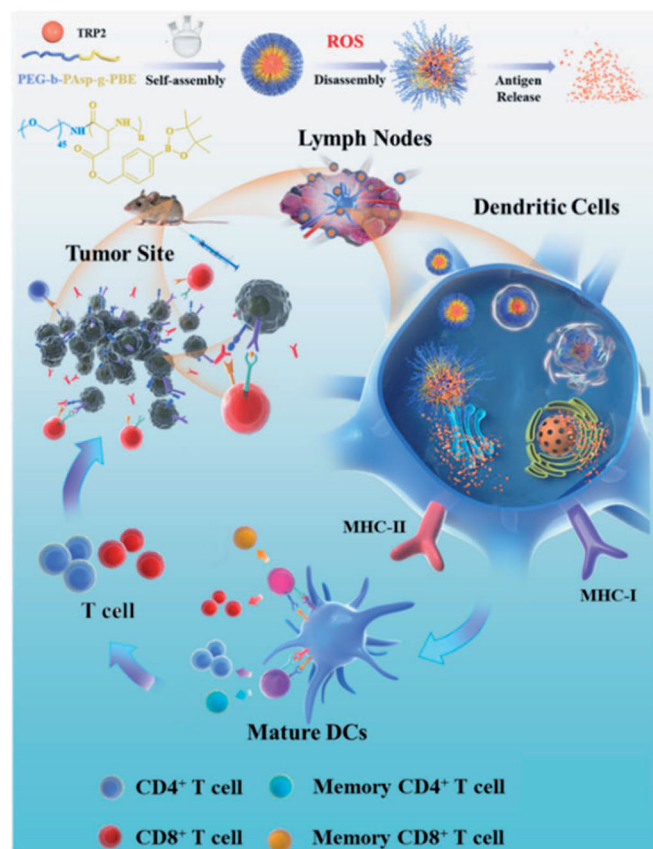
© 2022 The Author(s). Published by Informa UK Limited, trading as Taylor & Francis Group
This is an Open Access article distributed under the terms of the Creative Commons Attribution-NonCommercial License (<http://creativecommons.org/licenses/by-nc/4.0/>), which permits unrestricted non-commercial use, distribution, and reproduction in any medium, provided the original work is properly cited.

more efficient drainage to lymph node and optimal phagocytosis in DC (Gause et al., 2017; Riley et al., 2019). Therefore, it is cogent that effective delivery of nanocarrier could promote therapeutic efficacy in the immunotherapy.

PBE (phenylboronic ester) molecule can be selectively degraded by intracellular ROS (Reactive Oxygen Species) triggers, generating phenol and boronic acid as the oxidation products (Xu et al., 2016; Lu et al., 2017). In our previous work, we have synthesized PBE-modified copolymer with ring opening polymerization for accurate drug delivery and achieved excellent anti-tumor activity in HeLa cell (Wang et al., 2020). According to the fact that the level ROS in antigen presenting cell is also much higher, Broader's research group also constructed the aryl-boronate-modified dextran polymer with the ROS triggering property for antigen delivery to enhance ex-vivo immunotherapy efficiency (Manaster et al., 2019). Moreover, nanovaccine carried more negative charge through PBE modification because negatively charged tetravalent form of boronate ester structure was more stable at a physiological pH of 7.4 (Naito et al., 2018; Vrbata & Uchman, 2018). Additionally, PBE-modified nanovesicles can exhibited a typical pH-dependent manner, which could promote antigen cross-presentations when antigen escaped from the lysosomes into the cytoplasm. Therefore, PBE group is really useful to be applied in antigen delivery system, which attracted our considerable attention.

The polymer, as an optimized carrier, provide a biomedical platform for encapsulating tumor antigen and protecting them from degradation, which can accurately deliver sufficient doses of antigen to target the strongest antigen presenting cell, dendritic cell (DC). Based on our previous work, we here mainly extend the series of block copolymers with different molecular weight for optimization to achieve enhanced immunogenicity. The nanovaccine are self-assembled to form a core-shell structure including an anion copolymer (PAsp-g-PBE) in the inner core to encapsulate the tumor-associated antigen peptide derived from TRP2 (SVYDFVWL, an MHC-I restricted epitope) (Kakwere et al., 2017; Zeng et al., 2017; Zhang et al., 2017) through electrostatic interaction, and hydrophilic PEG outer layer to prolong blood circulation time. Through optimization, the candidate carrier PEG-b-PAsp-g-PBE with the proper block can transport TRP2 peptide to APC in lymph nodes efficiently and then loses its PBE side chains, leading to release of the preloaded TRP2 under the high level of ROS in DC cells. Also by the means of PEG-b-PAsp-g-PBE carrier, TRP2 tumor antigen is able to enhance cross-presentation, which facilitates endogenous antigen presenting via MHC-I for a cytotoxic T cell responses. Moreover, TRP2 tumor antigen could be accumulated in the draining lymph nodes for DC long-term antigen presentation with PEG-b-PAsp-g-PBE delivery.

As we all known, there are only a limited number of tumor vaccines capable of inducing optimal antitumor immunity without external adjuvant. Therefore, most of nanovaccines require co-delivering adjuvants for immunogenic improvement. For example, Zhang reported Fe_3O_4 /T-MPs nanovaccine with CpG/Lipo adjuvants can significantly suppress tumor growth and prolong survival (Zhao et al.,



Scheme 1. Schematic illustration of PEG-b-PAsp-g-PBE/TRP2 as a nanovaccine delivery system.

2019). However, undesired side effects, especially safety in adjuvants seriously hampered the clinical application, so it is urgent to look for the novel delivery platform without external adjuvants (Chesson et al., 2014; Mora-Solano et al., 2017). Here, it was exciting that we found PEG-b-PAsp-g-PBE/TRP2 nanovaccine without any external adjuvant did almost the same immunotherapeutic effect as that combined with CpG. It means that this nanovaccine could function as a robust platform with the simplified construction, achieving effective antigen delivery in cancer immunotherapy for wide application.

2. Materials and method

2.1. Synthesis and characterization of PEG-b-PAsp-g-PBE

The PEG-b-PAsp-g-PBE copolymer was synthesized via the amine-initiated ring-opening polymerization (ROP) and esterification reaction. With different molar ratio between BLA-NCA and m-PEG-NH₂, we obtained different block copolymers with different molecular weight. According to the length of PAsp chain, PBE with proper molar ratio was added into reaction solution and we get PEG-b-PAsp-g-PBE with different grafting degree (Yang et al., 2015; Hu et al., 2017; Wang et al., 2020). ¹H NMR spectra of the polymers were recorded on a Bruker 400 MHz nuclear magnetic resonance instrument using D₂O as the solvents. Gel permeation chromatography (GPC) was used to analyze the molecular

weights and molecular weight distributions (M_w/M_n) of the polymers. GPC of polymer (PEG-b-PAsp and PEG-b-PAsp-g-PBE) was measured by a Waters 1525 chromatograph equipped with a Waters 2414 refractive index detector.

2.2. Cell Lines and culture conditions

B16F10(Mouse skin melanoma cells) and LO2 (Human normal liver cells) cell lines were provided by Chinese Academy of Sciences Cell Bank and maintained in Dulbecco's Modified Eagles Medium (DMEM) containing 10% fetal bovine serum (HyClone Laboratories, Inc. Logan, UT, USA) with 100 units mL^{-1} penicillin, and 100 mg mL^{-1} streptomycin. The cells were cultured in a humidified incubator at 37 °C, 5% CO_2 . The cell culture medium was changed every 48 h.

Bone marrow-derived dendritic cells (BMDCs) were obtained from the bone marrow of 6–8 weeks old C57BL/6 mice. The bone marrow cells were flushed out of the femurs and tibias with RPMI 1640, passed through a cell strainer and treated with red blood cell lysis solution to obtain single cell suspensions. Then, BMDCs were suspended in complete RPMI 1640 medium containing 10% fetal bovine serum (FBS), GM-CSF (10 ng/mL) and IL-4 (10 ng/mL) in six-well plates at 37 °C. On day 3, the culture medium was replaced by 4 mL fresh medium containing GM-CSF. On day 7, most of the cells were differentiated into BMDCs and ready for use (Dong et al., 2019; 2019; Zhao et al., 2019).

Male C57BL/6 mice weighing 18–20 g furnished by Experimental Animal Center, Jiangsu Academy of Traditional Chinese Medicine. All animal procedures were performed in accordance with the Guidelines for Care and Use of Laboratory Animals of China Pharmaceutical University and approved by the Animal Ethics Committee of China Pharmaceutical University, Jiangsu, China.

2.3. In vitro cytotoxicity of copolymers

The cytotoxic effect of PEG-b-PAsp and PEG-b-PAsp-g-PBE was evaluated using MTT according to a previous protocol. Briefly, BMDC were initially seeded into a 96-well cell culture plate at 8×10^3 per well and then incubated for 24 h at 37 °C under 5% CO_2 . Then, 1640 RPMI solutions with 10% FBS of PEG-b-PAsp and PEG-b-PAsp-g-PBE at different concentrations were added under the same condition for 72 h incubation. Four hours before stopping the experiment, culture medium was replaced with MTT solution of 0.2 mL . At the end of the experiment, the medium solution was replaced by 0.15 mL DMSO solution. The optical density of the solution was measured by enzyme linked immunosorbent assay (ELISA) at a wavelength of 490 nm. The absorbance value of untreated cells was set at 100%. Each experiment was repeated three times in sextuplicate. The cell viability was calculated according to following formula: the viability (%) = $(\text{OD}_{\text{exp}} - \text{OD}_{\text{blank}})/(\text{OD}_{\text{control}} - \text{OD}_{\text{blank}}) \times 100\%$ (Li et al., 2017).

2.4. Preparation and characterization of PEG-b-PAsp-g-PBE/TRP2 nanovaccine

The PEG-b-PAsp/TRP2, PEG-b-PAsp-g-PBE/TRP2 nanovaccine were prepared by dialysis method. TRP2 peptide (20 mg) and PEG-b-PAsp-g-PBE (50 mg) were dissolved in deionized water (15 mL) (John et al., 2013). The above solution was stirred at room temperature for 6 h. The mixture was dialyzed against deionized water to remove free TRP2 peptide. The solution in the dialysis bag was lyophilized to obtain PEG-b-PAsp-g-PBE/TRP2 micelles. PEG-b-PAsp/TRP2 was prepared by the same method.

Drug loading content (DLC) were detected by BCA kit and calculated according to the following formula (Chesson et al. 2014; Wang et al., 2019; Bu et al., 2020; Chen et al., 2019):

$$\text{DLC} (\%) = (\text{weight of loaded drug}/\text{weight of NTs}) \times 100\%^{47-49}.$$

The size and zeta potential of polymeric micelles were measured by dynamic light scattering (DLS) using a Malvern ZS90 instrument equipped with a 532 nm laser at a scattering angle of 90°. The measurements were performed at 25 °C after diluting the samples to an appropriate concentration with ultrapure water (pH= 7.0) (Hu et al., 2020).

The morphology of nanovaccine was observed by Transmission Electron Microscopy (TEM) on a JEOL-2100 with accelerating voltage of 200 kV. TEM samples were prepared by drop-casting dispersion onto copper grids covered by carbon film.

In vitro release behavior of ROS-triggered TRP2 load vaccine was measured by fluorescence analysis. In order to detect the concentration of TRP2, the TRP2 peptide was labeled with CY3 through amido bond. CY3 labeled TRP2 (CY3-TRP2) was synthesized by mixing CY3-NHS with TRP2 at the proper molar ratio for 12 h under stirring in the dark, purified by dialysis method and obtained by lyophilization. PEG-b-PAsp/CY3-TRP2 and PEG-b-PAsp-g-PBE/CY3-TRP2 was fabricated according to the above method. 2 mg of PEG-b-PAsp/CY3-TRP2 and PEG-b-PAsp-g-PBE/CY3-TRP2 aqueous solution was infused into a dialysis bag with 3500 DA cutoff and dialyzed against phosphate-buffered saline (PBS, 1 mM H_2O_2) at 37 °C on an orbital shaker in the dark. At each interval time over a period of 48 h (1 h, 2 h, 4 h, 6 h, 10 h, 12 h, 24 h, 48 h), the concentration of CY3-TRP2 in the dialysate was measured by fluorescence analysis. The total volume of dialysis medium was maintained at 80 mL through the test (Wang et al., 2020).

2.5. In vitro immunization studies

2.5.1. Antigen uptake and localization of nanovaccine in BMDCs

To investigate cellular uptake and localization of nanovaccine in BMDCs, flow cytometry CLSM was applied. BMDC was cultured into a 6 well plate. After being treated with PEG-b-PAsp/FITC-TRP2, PEG-b-PAsp-g-PBE/at 37 °C for 30 min, cells were collected and stained with CD11c PBS. The percentage

of cells internalized with nanovaccine was analyzed by flow cytometry (Liu et al., 2019; Zhao et al., 2019).

Subsequently, CLSM was applied to investigate the general intracellular distribution. In brief, BMDC was seeded on a coverslip in 35 mm dishes and incubated with FITC-TRP2, PEG-b-PAsp/FITC-TRP2, PEG-b-PAsp-g-PBE/FITC-TRP2. After culturing for 30 min, the cells were washed several times with PBS to remove the remaining samples and dead cells. At last, cell nuclei were stained with DAPI (2 µg/mL) for 15 min and fluorescent images were recorded by a CLMS.

2.5.2. Maturation of BMDCs and cross-presentation of antigens

To determine whether PEG-b-PAsp-g-PBE/TRP2 nanovaccine treatment could activate DC mature in vitro, flow cytometry and ELISA kits was employed in this experiment. Immature BMDCs were incubated with PEG-b-PAsp-g-PBE, free TRP2, PEG-b-PAsp/TRP2 and PEG-b-PAsp-g-PBE/TRP2 (50 µg TRP2 per cell) for 24 h, followed by being stained with a mixture of antibodies labeled with different fluorescent dyes against CD11c, CD80, CD86, MHC-I, CCR-7. Membrane CD80, CD86, CCR-7 on CD11c+DCs were analyzed by a MACSQuant™ flow cytometry. Concentrations of Interleukin-1β (IL-1β), interleukin-6 (IL-6), tumor necrosis factor alpha (TNF-α) in culture supernatants were measured by ELISA kits according to vendor's protocol. All samples were measured in triplicate (Rajput et al., 2018; Hu et al., 2020; Li et al., 2020).

2.5.3. T cell proliferation

For T cell proliferation assay, splenic T cells from C57BL/6 male mice, selected by flow cytometry, were stained by CFSE Cell Proliferation Kit (CFSE, Invitrogen) under the vendor's instructions. Then, the BMDCs were treated with TRP2, PEG-b-PAsp/TRP2, PEG-b-PAsp-g-PBE/TRP2 and incubated with splenic T cells at the cell number ratio of 1:5, 1:10 for 72 h. The T cells proliferation was finally analyzed by flow cytometry after staining CD3, CD4, CD8. Concentrations of interferon-gamma (IFN-γ) in culture supernatants were measured by ELISA kits according to the above method (Kapadia et al., 2016; Dixit et al., 2018; Wang et al., 2018; Zupancic et al., 2018).

2.6. In vivo immunization study

2.6.1. In vivo fluorescence imaging

The fluorescence imaging in vivo was determined by imaging system (Tanon ABL X8). CY3-TRP2, PEG-b-PAsp/CY3-TRP2, PEG-b-PAsp-g-PBE/CY3-TRP2 (containing same concentration of CY3-TRP2) was injected subcutaneously near LNs of C57BL/6 mice with hair removed. An in vivo imaging system using 532 nm as the excitation wavelength and 560–750 nm as the emission range was utilized to obtain CY3-TRP2 signal. For in vivo tracking, the fluorescence signals of LNs were detected at different time from 0 h to 48 h (Wu et al., 2019).

2.6.2. CTL response analysis

C57BL/6 male mice were immunized with PBS, PEG-b-PAsp-g-PBE, TRP2, PEG-b-PAsp/TRP2 and PEG-b-PAsp-g-PBE/TRP2 (containing same concentration of TRP2) by injecting. The vaccination was performed three times every 7 days as interval (at day 0, 7, and 14). Mice were sacrificed after 20 days. The spleen and serum were collected for immunological response analysis. Percentage of T cell subtypes (CD4⁺ T cell and CD8⁺ T cell) in spleen was evaluated by flow cytometry (Guo et al., 2015).

2.6.3. Memory T-cell response analysis

To further evaluate memory T-cell responses, splenocytes were restimulated with TRP2 (50 µg/mL) for 72 h and subsequently stained with CD3, CD4, CD8, CD44 and CD62L. Subsequently, the flow cytometer was used to analyze percentage of memory T-cells in splenocytes (Liu et al., 2016; Zhang et al., 2019; Shae et al., 2020).

2.7. Tumor prevention

For tumor prevention, after the completion of three vaccinations, 8×10^5 B16F10 cells (suspended in 100 µL sterile PBS) were subcutaneously injected into the right side of the flank. The tumor volume was calculated by length \times width \times height \times 0.5. The tumor sizes were measured every 3 days by a digital caliper. Eighteen days later, tumor-bearing mice were sacrificed, and the tumor tissues were removed from the bodies for measurement. Major organs (heart, liver, spleen, lung and kidney) were dissected from mice and hematoxylin-eosin (H&E) staining. T cell subtypes analysis was performed at the end of experiment according to previous protocol (Rajput et al., 2018; Zhao et al., 2019).

2.8. Antitumor efficacy study

Antitumor efficacy study was conducted when the tumor average volume reached 80–100 mm³. On day 5, the mice were divided into seven groups vaccinated with PBS, PEG-b-PAsp-g-PBE, αPD-1, TRP2, PEG-b-PAsp/TRP2 and PEG-b-PAsp-g-PBE/TRP2 (containing same concentration of TRP2) on day 5, 10 and 15. Tumor sizes were measured every 3 days and the percentage of mouse survival rate was calculated at the same time. The spleens were collected for immunological response analysis at the end of experiment. Splenocytes were stained with CD3, CD4, CD25, FOXP3 and percentage of T regular cells in spleen were evaluated by flow cytometry. Hematoxylin-eosin (H&E) and immunofluorescence staining were also carried out at the same time (Zhang et al., 2019; Zhao et al., 2019).

3. Results and discussion

3.1. Synthesis and characterization of PEG-b-PAsp-g-PBE

Ring Opening Polymerization (ROP) was employed to synthesize polymer PEG-b-PAsp, explored in our previous research.

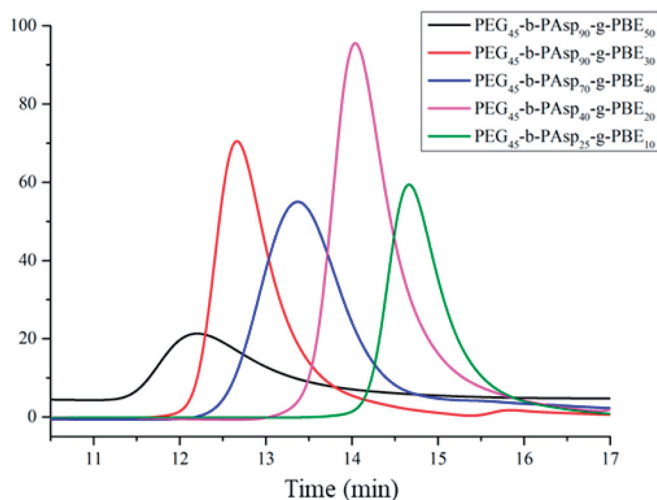


Figure 1. Gel permeation chromatography (GPC) of copolymers PEG-b-PAsp-g-PBE.

On this base, by varying the feed molar ratio of monomer (BLA-NCA) to macromolecular initiator (PEG-NH₂), copolymers PEG-b-PAsp with different molecular weight were synthesized. As the polymerization degrees increased to 90, the length of PAsp chain did not increase obviously. So under this reaction condition, we obtained four copolymers PEG₄₅-b-PAsp_n ($n = 25, 40, 70, 90$) for further experiments. Subsequently, the PBE group was grafted to PAsp chain by ester bond, which endow the resulting polymer with ROS-responsive feature. The structure of the copolymer (PEG-b-PAsp-g-PBE and PEG-b-PAsp) was characterized using ¹H-NMR spectroscopy (Figures S1 and S2) and GPC traces (Figures S3 and 1). The compositions of PEG-b-PAsp and PEG-b-PAsp-g-PBE diblock polymers were listed in Tables S1 and S2. These results showed that we successfully synthesized series of copolymer (PEG-b-PAsp-g-PBE and PEG-b-PAsp) with different molecular weight.

Cytotoxicity of the polymer (PEG-b-PAsp and PEG-b-PAsp-g-PBE) against BMDC cells and LO2 was respectively evaluated by MTT assay in this study. The Polymer-treated (PEG-b-PAsp and PEG-b-PAsp-g-PBE) cells showed a dramatically high cell viability (>85%) over a wide concentration range (15–300 μg/mL) (Figures S4–S7). Inspired by its low cytotoxicity, we carry out the further experiments with PEG-b-PAsp-g-PBE.

3.2. Preparation of nanovaccine and morphology study

The PEG-b-PAsp/TRP2 and PEG-b-PAsp-g-PBE/TRP2 nanovaccine were prepared by dialysis method through the electrostatic interaction. The morphology study of nanovaccine was characterized by dynamic light scattering (DLS) and transmission electron micrographs (TEM) measurements. The hydrodynamic size of PEG₄₅-b-PAsp₉₀/TRP2 and PEG₄₅-b-PAsp₉₀-g-PBE₅₀/TRP2 are around 100 and 110 nm (Figure S8). Also after incubated with 10% FBS, nanovaccine show no clear changes in the hydrodynamic size (Figure S9). The zeta potential of PEG-b-PAsp/TRP2 micelles decreased with the PAsp chain increase (Table S3). Also PEG-b-PAsp-g-PBE/TRP2 nanovaccine carried more negative

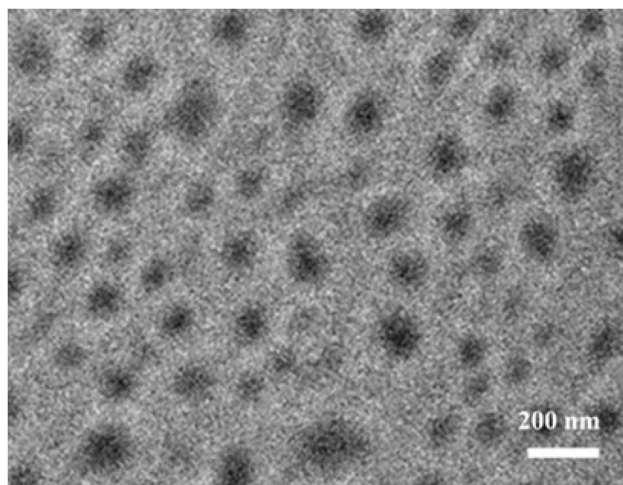


Figure 2. TEM image of PEG₄₅-b-PAsp₉₀-g-PBE₅₀/TRP2.

charge, which can further confirm the PBE group has been modified successfully. Negatively charged tetravalent form of boronate ester structure was more stable at a physiological pH of 7.4. The morphologies of the nanoparticles PEG₄₅-b-PAsp₉₀-g-PBE₅₀/TRP2 were observed as well-dispersed spherical micelles around 90 nm (TEM), which is proper for lymph nodes drainage and DC uptake (Figure 2).

We next assessed drug loading efficiency of PEG-b-PAsp/TRP2 and PEG-b-PAsp-g-PBE/TRP2 nanovaccine by BCA analysis. According to DLE the following formula, the calculation of drug loading efficiency was listed in Table S4. As the increase of PAsp chain, more TRP2 peptide has been encapsulated into nanoparticle through the electrostatic interaction. PBE modification did not significantly affect drug loading efficiency of nanocarrier. These results showed that we successfully construct series of nanovaccine with different molecular weight, surface charge and drug loading efficiency for later optimization.

In order to study *in vitro* TRP2 release behavior of the micelles, we labeled TRP2 with CY3, then fabricated PEG-b-PAsp/CY3-TRP2 and PEG-b-PAsp-g-PBE/CY3-TRP2 nanovaccine, monitoring CY3-TRP2 by fluorescence analysis. The fluorescence emission spectroscopy showed that we successfully labeled TRP2 with TRP2 (Figure S10). To mimic the conditions of lysosomes, microenvironment in DC and normal physiological, the micelles were incubated with PBS, including a control level (pH = 7.4), an acidic pH level (pH = 5.0) and an acidic pH level with ROS (pH = 5.0 with 1 mM H₂O₂). Both PEG-b-PAsp/CY3-TRP2 and PEG-b-PAsp-g-PBE/CY3-TRP2 performed a sustained release process and the controlled release behavior. As shown in Figure 3, the release of CY3-TRP2 from PEG-b-PAsp/CY3-TRP2 and PEG-b-PAsp-g-PBE/CY3-TRP2 was low (29% and 31%) at normal physiological pH 7.4 after 48 h incubation. Addition with 1 mM H₂O₂ in phosphate-buffered saline, the release rate of PEG-b-PAsp-g-PBE/CY3-TRP2 increased to 40%, because PBE group can response to ROS trigger and cause nanovaccine being cleavable and drug releasing. Acidification of the buffer to pH 5.0 caused a moderately higher release rate (35% and 41%), owing to the simulated lysosomes under the similar pH condition breaking

the electrostatic interaction of nanovaccine and causing solubility of TRP2 increase. Moreover, compared with PEG-b-PAsp/CY3-TRP2, a significantly higher release rate (77%) of CY3-TRP2 from PEG-b-PAsp-g-PBE/CY3-TRP2 was measured at acidic pH level with H_2O_2 addition after 48 h incubation (Figure 3). Therefore, dual-triggered (ROS and pH) degradation of platform can cause the dissociation of nanovaccine and TRP2 antigen released.

3.3. In vitro immunization studies

3.3.1. Antigen uptake and distribution

Nanovaccine with different molecular weight uptake was quantified using the technique of flow cytometric analyses. Results showed that the PEG-b-PAsp-g-PBE/FITC-TRP2 were

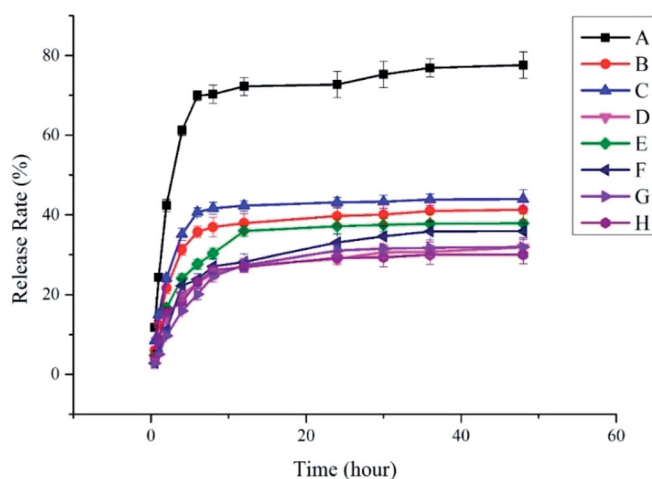


Figure 3. In vitro release profiles of CY3-TRP2 (A PEG-b-PAsp-g-PBE/CY3-TRP2 at pH = 5.0 with 1 mM H_2O_2 ; B PEG-b-PAsp-g-PBE/CY3-TRP2 at pH = 5.0; C. PEG-b-PAsp-g-PBE/CY3-TRP2 at pH = 7.4 with 1 mM H_2O_2 ; D. PEG-b-PAsp-g-PBE/CY3-TRP2 at pH = 7.4; E. PEG-b-PAsp/CY3-TRP2 at pH = 5.0 with 1 mM H_2O_2 ; F. PEG-b-PAsp/CY3-TRP2 at pH = 5.0; G. PEG-b-PAsp/CY3-TRP2 at pH = 7.4 with 1 mM H_2O_2 ; H. PEG-b-PAsp/CY3-TRP2 at pH = 7.4). Results are presented as mean (SD) ($n = 3$) (* $P < .05$).

carried into the BMDC cell lines at the highest uptake of about 98.3%, in comparison with other PBE modification nanovaccine containing with same amount of nanocarrier. The capability of antigen uptake was enhanced with the molecular weight increased, due to its highly negative surface charge and drug loading efficiency. Also the PEG-b-PAsp/FITC-TRP2 was in the same situation (Figure S11A). Consistent with this result, confocal fluorescence imaging showed BMDC treated with PEG-b-PAsp/TRP2 and PEG-b-PAsp-g-PBE/TRP2 appeared significantly higher TRP2 signal (green) than that of other control groups (Figure S11B). Considering copolymers cellular uptake, we finally chose PEG₄₅-b-PAsp₉₀/TRP2 and PEG₄₅-b-PAsp₉₀-g-PBE₅₀/TRP2 as the nanovaccine to carry out the further experiments.

The intracellular localization of TRP2 peptide in BMDCs was evaluated by confocal laser microscopy, following with nucleus and lysosome stained by DAPI and lysotracker red respectively. According to above experiment, PEG-b-PAsp/TRP2 and PEG-b-PAsp-g-PBE/TRP2 containing same concentration of TRP2 was incubated BMDC for 30 min. Figure 4 showed the green signal of TRP2 (green) was co-localized with lysosomes (red), indicating the cellular uptake and endosomal escape of tumor antigen by BMDC. A small proportion of TRP2 could be captured the DCs in group treated with TRP2 only. TRP2 signal from the PEG-b-PAsp/TRP2 group increased marginally in the cytoplasm of BMDCs, compared to free TRP2. However, BMDC treated with PEG-b-PAsp-g-PBE/TRP2 exhibited the strongest fluorescence signal, indicating more effectively delivery. The quantitative data was detected by flow cytometry, further exploring that the mean fluorescence intensities of nanovaccine after 30 min incubation. The FCM results (Figure S12) were basically consistent with the CLMS results, indicating TRP2 released from the PEG-b-PAsp-g-PBE/TRP2 were quickly transported to the cytoplasm in response to high concentration of ROS in BMDCs. All of the above results illustrated the efficient cellular uptake of nanovaccine with PBE modification. Moreover, the TRP2 escaped from the lysosomes into the cytoplasm of

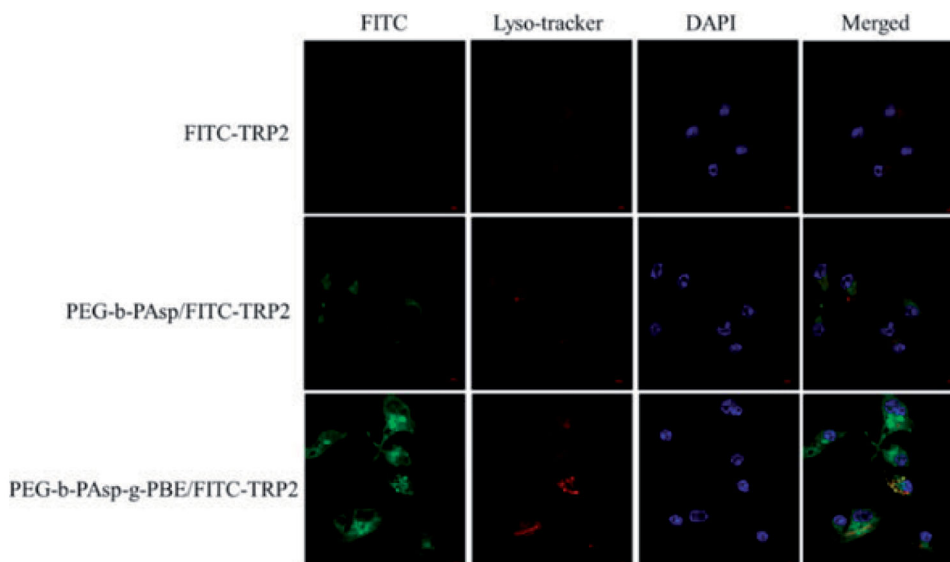


Figure 4. Cellular uptake and intracellular localization of TRP2, PEG₄₅-b-PAsp₉₀/TRP2 and PEG₄₅-b-PAsp₉₀-g-PBE₅₀/TRP2 in BMDC cells.

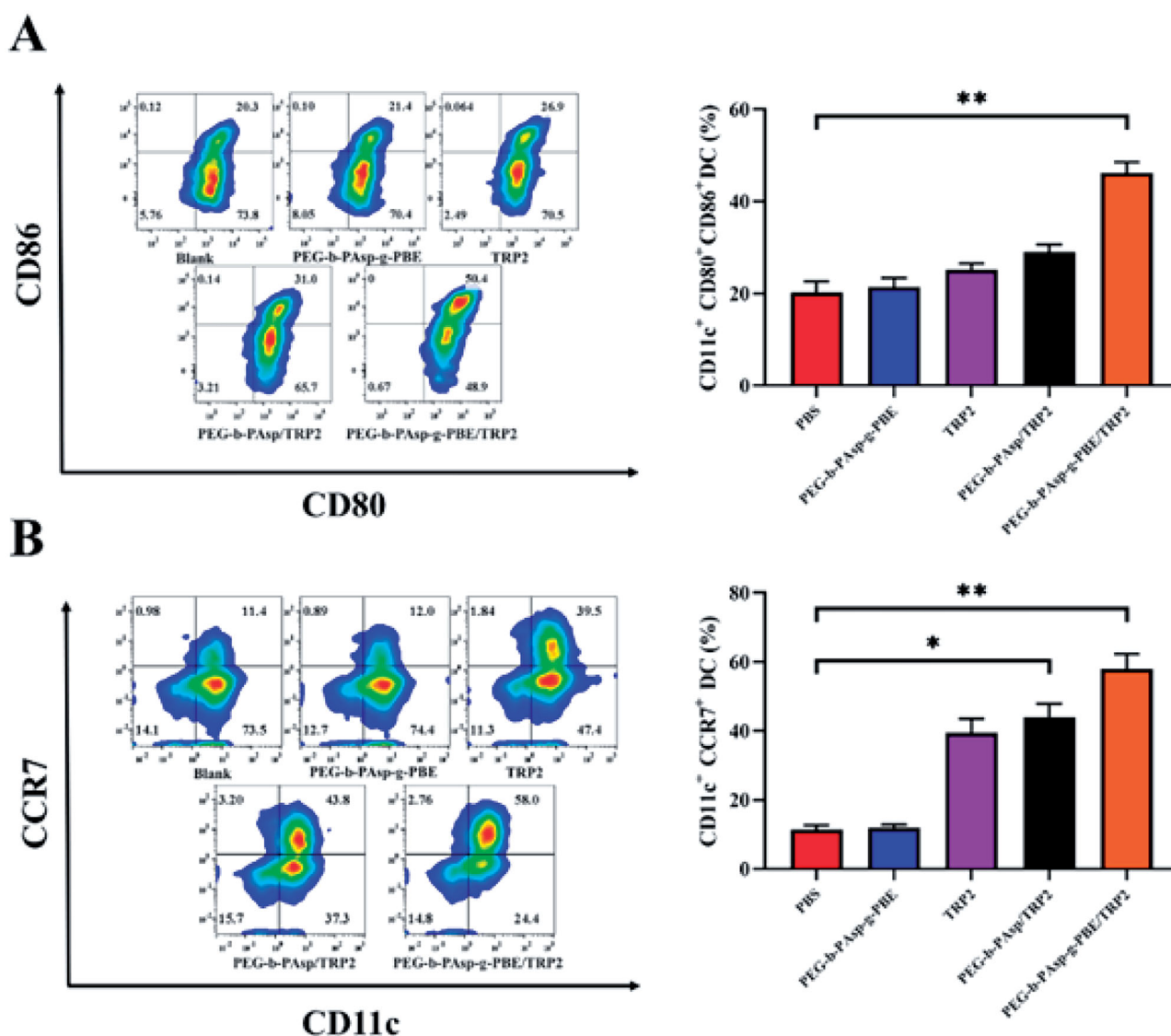


Figure 5. In vitro DC maturation, and antigen cross-presentation triggered by PEG-b-PAsp-g-PBE/TRP2 nanovaccine. (A, B) The representative flow cytometry images and statistic data of DC maturation for DCs treated with nanovaccine CD11c⁺, CD80⁺, CD86⁺, CCR7⁺ are the markers for matured DCs. Results are presented as mean (SD) ($n = 5$) (* $P < .05$ and ** $P < .01$).

BMDCs, suggesting that tumor antigens delivered by nanoparticle may be presented through both the MHC-I and MHC-II pathways.

3.3.2. Maturation of BMDCs and cross-presentation of antigens

DCs as the strongest antigen presenting cells are responsible for activating the immune responses. After capturing tumor antigen, immature DC will become mature DCs to present the antigen into nearby draining lymph nodes. The level of DC maturation is quite an important prerequisite for evaluating the immune response in DC-based nanovaccine.

It is well known that the co-stimulatory molecules (CD80, CD86) on the cell membrane would be some typical markers of mature DC. Therefore, the DCs maturation was assessed by detecting CD80 and CD86 level. In comparison to control group, the percentage of CD80⁺ CD86⁺ DCs was significantly higher in the group treated by PEG-b-PAsp-g-PBE/TRP2

(Figure 5(A)). Also the level of CCR7 expression on DC was dramatically improved (50%) in the PEG-b-PAsp-g-PBE/TRP2 treated group, with 5 folder higher than blank control, whereas 27% and 35% in the TRP2-treated and PEG-b-PAsp/TRP2-treated group (Figure 5(B)). Consistent with the result, BMDCs treated with PEG-b-PAsp-g-PBE/TRP2 had a significantly higher level of IL-1 β , IL-6 and TNF- α than the other control groups in the cytokine measurement by ELISA assays (Figure S13). We all know cytokine TNF- α , IL-1 β and IL-6 secreted from BMDCs plays an important role in T-cell proliferation and CTL activation. Taken together, all these results indicate that TRP2 nanovaccine modified with PBE could activate BMDCs and induce an enhanced immunological effect in vitro without external adjuvant.

3.3.3. T cell proliferation

Specific CD4⁺ and CD8⁺ T cells proliferation is one of the most important indexes to evaluate the vaccine-induced

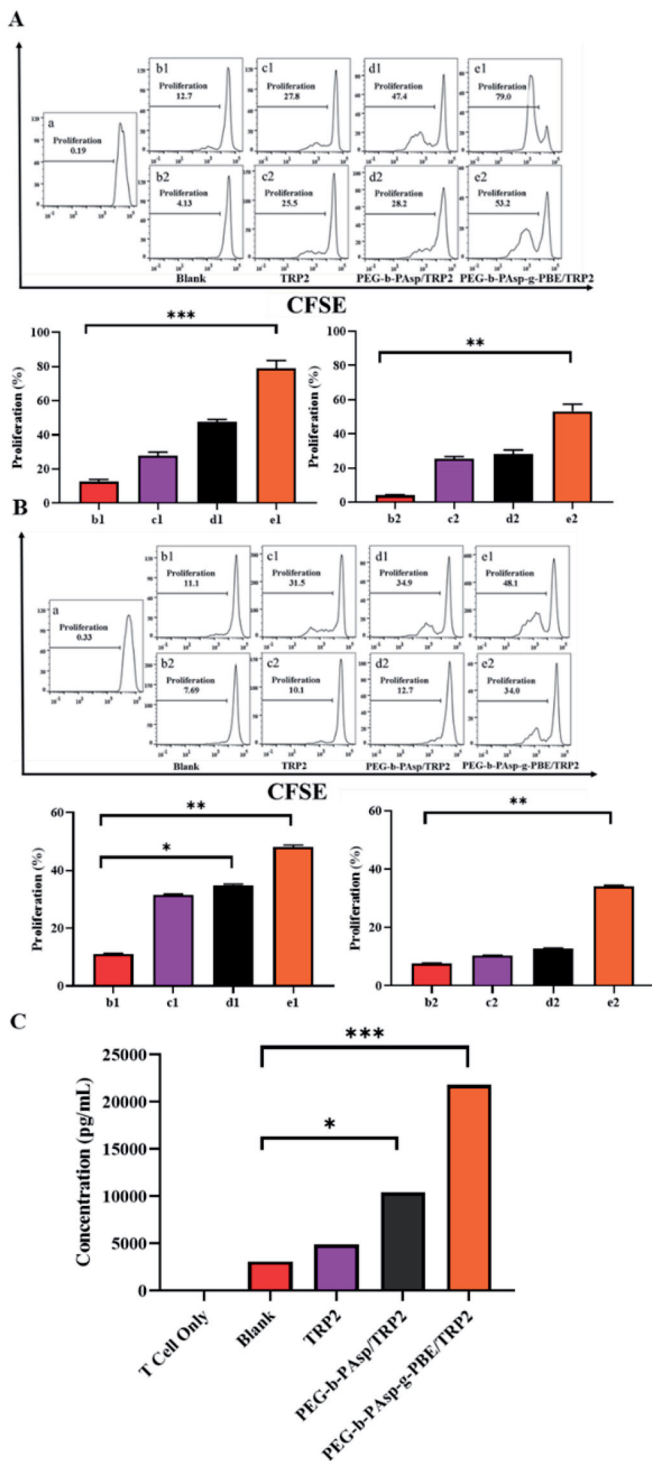


Figure 6. T cell proliferation and IFN- γ secretion. (A, B) The representative flow cytometry images and statistic data analysis of (A) CFSE-labeled CD8⁺ T cell and (B) CFSE-labeled CD4⁺ T cell proliferation in spleen; (C) IFN- γ cytokine secreted from T cell after treated with nanovaccine. Results are presented as mean (SD) ($n = 5$) (* $p < .05$, ** $p < .01$ and *** $p < .001$).

immune response (Figure 6(A,B)). We pulsed DCs with nanovaccine (TRP2, PEG-b-PAsp/TRP2, PEG-b-PAsp-g-PBE/TRP2) in vitro, followed by incubating them with CFSE-labeled T cells. All group pulsed with DCs exhibited fingerlike peaks, whereas untreated group showed no changes. As the DC ratio increased, the proliferative responses exhibited different level of increase in each group. Moreover, T cells treated

with PEG-b-PAsp-g-PBE/TRP2-pulsed DCs showed the distinct proliferation capability in all groups, due to its highest proliferation index and lower CFSE signals similar to that of the blank control. Meanwhile, PEG-b-PAsp/TRP2 and TRP2 group only showed the moderate proliferative responses compared to the group of DC pulsed only. To further verify T cell proliferation and activation by PEG-b-PAsp-g-PBE/TRP2 in vitro, the IFN- γ secretion from T cell was also analyzed by ELISA. The PEG-b-PAsp-g-PBE/TRP2 nanovaccine could induce much more IFN- γ secretion than any other groups, nearly 300 folds higher than untreated group (Figure 6(C)). It was uncovered that nanovaccine PEG-b-PAsp-g-PBE/TRP2 without any external adjuvant could obviously enhance T cell proliferation capability and trigger stronger immune responses in vitro.

3.4. In vivo immunization studies

3.4.1. Nanovaccine promoted retention in draining lymph nodes

Efficient delivery of antigens could exert a strong immune response against tumor occurrence. To determine if nanovaccine can delivery tumor antigen into draining lymph nodes, where DC maturation and cross-presentation would take place, a live animal imaging system was exploited for accurate monitoring in the experiment. Mice were injected with CY3-TRP2, PEG-b-PAsp/CY3-TRP2, PEG-b-PAsp-g-PBE/CY3-TRP2 (containing same concentration of CY3-TRP2) for in vivo fluorescence imaging. As shown in Figure 7, CY3-TRP2 fluorescence signals could be observed very strong near popliteal lymph nodes after a few minutes' injection. At 4 h post-injection, fluorescence signals in groups of CY3-TRP2 and PEG-b-PAsp/CY3-TRP2 decreased sharply only 2% retention in lymph nodes due to its easy degradation. In contrast, PEG-b-PAsp-g-PBE/CY3-TRP2 nanovaccine exhibited obviously enhanced (8 folders) retention in lymph nodes. Moreover, 12 h later fluorescence intensity of CY3-TRP2 and PEG-b-PAsp/CY3-TRP2 was very low, while the concentration of TRP2 in PEG-b-PAsp-g-PBE/CY3-TRP2 was clearly detected even after 48 h (Figure 7). The above results evidenced that PEG-b-PAsp-g-PBE/CY3-TRP2 could be accumulated in the draining lymph nodes for DC long-term antigen presentation, which can achieve enhanced immunogenic.

3.4.2. CTL response analysis

The CD3⁺CD8⁺ T cell, called cytotoxic T lymphocytes (CTLs), can directly kill cancer cells. Therefore, the percentage of CD8⁺ T cell subset is a significant indicator of immune response in vivo. After the boosting immunization, we collected splenocytes from each treated group of vaccinated mice (PBS, PEG-b-PAsp-g-PBE, TRP2, PEG-b-PAsp/TRP2 and PEG-b-PAsp-g-PBE/TRP2) and stained with APC-CD8 and PE-CY7-CD3 antibody. The CTL response in PBS and PEG-b-PAsp-g-PBE carrier treated groups are at the same level, only 11.2% and 12.7% respectively. However, PEG-b-PAsp-g-PBE/TRP2 nanovaccine significantly improved the percentage of CD8⁺T cells (26.7%) more than TRP2 (16.7%) and PEG-b-PAsp/TRP2 (17.1%). Statistical analysis indicated that

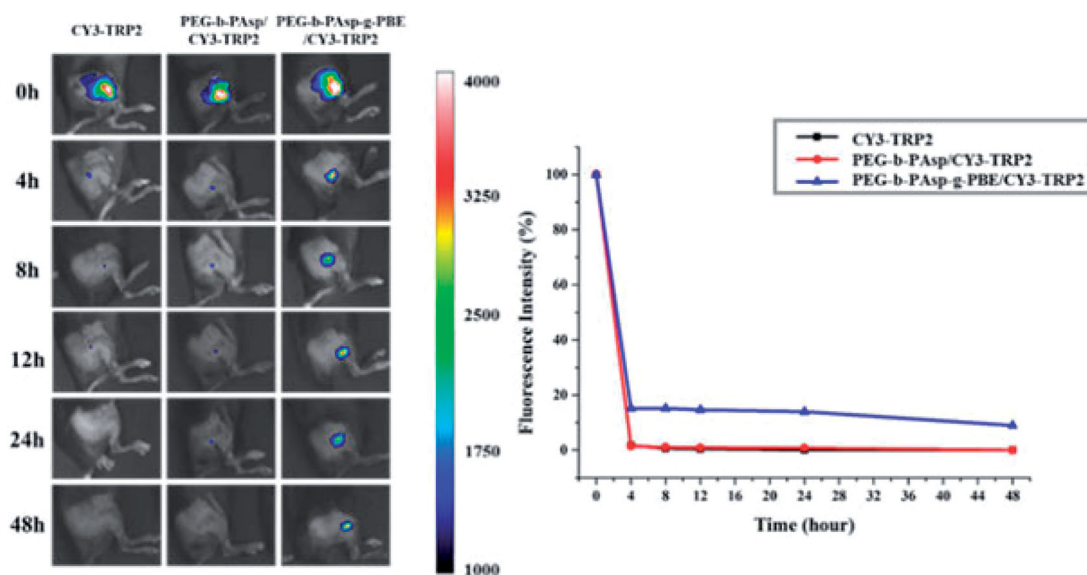


Figure 7. In vivo fluorescence images and quantified fluorescence signals at the lymph nodes at different time points after injecting free CY3-TRP2, PEG-b-PAsp/CY3-TRP2 or PEG-b-PAsp-g-PBE/CY3-TRP2 nanovaccine.

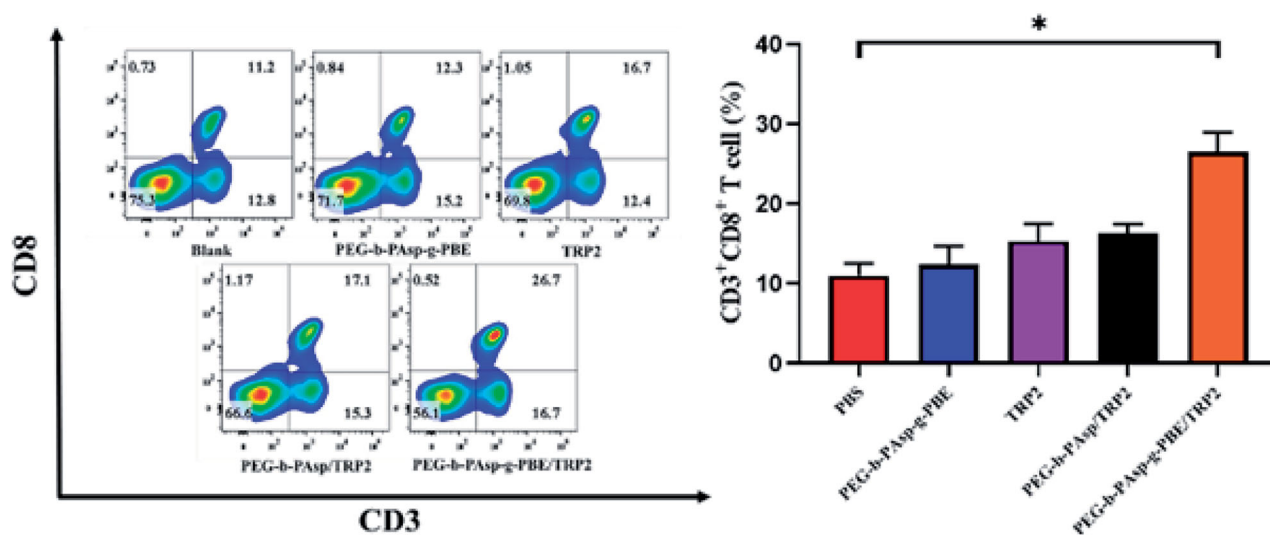


Figure 8. The representative flow cytometry images and statistic data of CD8⁺ T cells in the spleen from mice immunized with nanovaccine. Results are presented as mean (SD) ($n = 5$) (* $P < .05$).

adjuvant-free TRP2 nanovaccine with PBE modification can elicit more efficiently CTLs responses than TRP2 and PEG-b-PAsp/TRP2 (Figure 8).

3.4.3. Memory T-cell response analysis

As we all known, memory T-Cell play a vital role in developing a long-term protection to fight against the second attack of pathogen infection. So, we tested the induction of memory T cells in restimulated splenocyte from vaccinated mice. Memory T cells are classified to central memory T cell (TCM) and effector memory T cells (TEM). TCM, highly expressing molecule CD62L, showed higher antitumor activities than TEM. After restimulating, these cells were stained by CD44-APC, CD62L-PE to analyze percentage of TCM. As shown in, PEG-b-PAsp-g-PBE/TRP2 group showed significant increase (10%) in the CD8⁺ TCM population (CD8⁺CD44⁺

CD62L⁺), compared with untreated mice. In contrast, treatment with TRP and PEG-b-PAsp/TRP2 induced the generation of slightly more (2.4%, 3.9%) TCM than vaccination with PBS group. Similarly, in CD4⁺ TCM analysis, PEG-b-PAsp-g-PBE/TRP2 group elicited significantly higher central memory T cells than other groups (Figure 9). Taken together, typical flow cytometry results of PEG-b-PAsp-g-PBE/TRP2 adjuvant-free nanovaccine can induce the strong memory T-cell immune response for long-term prevention against tumors.

3.5. Tumor prevention

To investigate the in vivo prophylactic effect, mice were divided into five groups (PBS, PEG-b-PAsp-g-PBE, TRP2, PEG-b-PAsp/TRP2 and PEG-b-PAsp-g-PBE/TRP2) and vaccinated before tumor cell implanted and then tumor sizes were

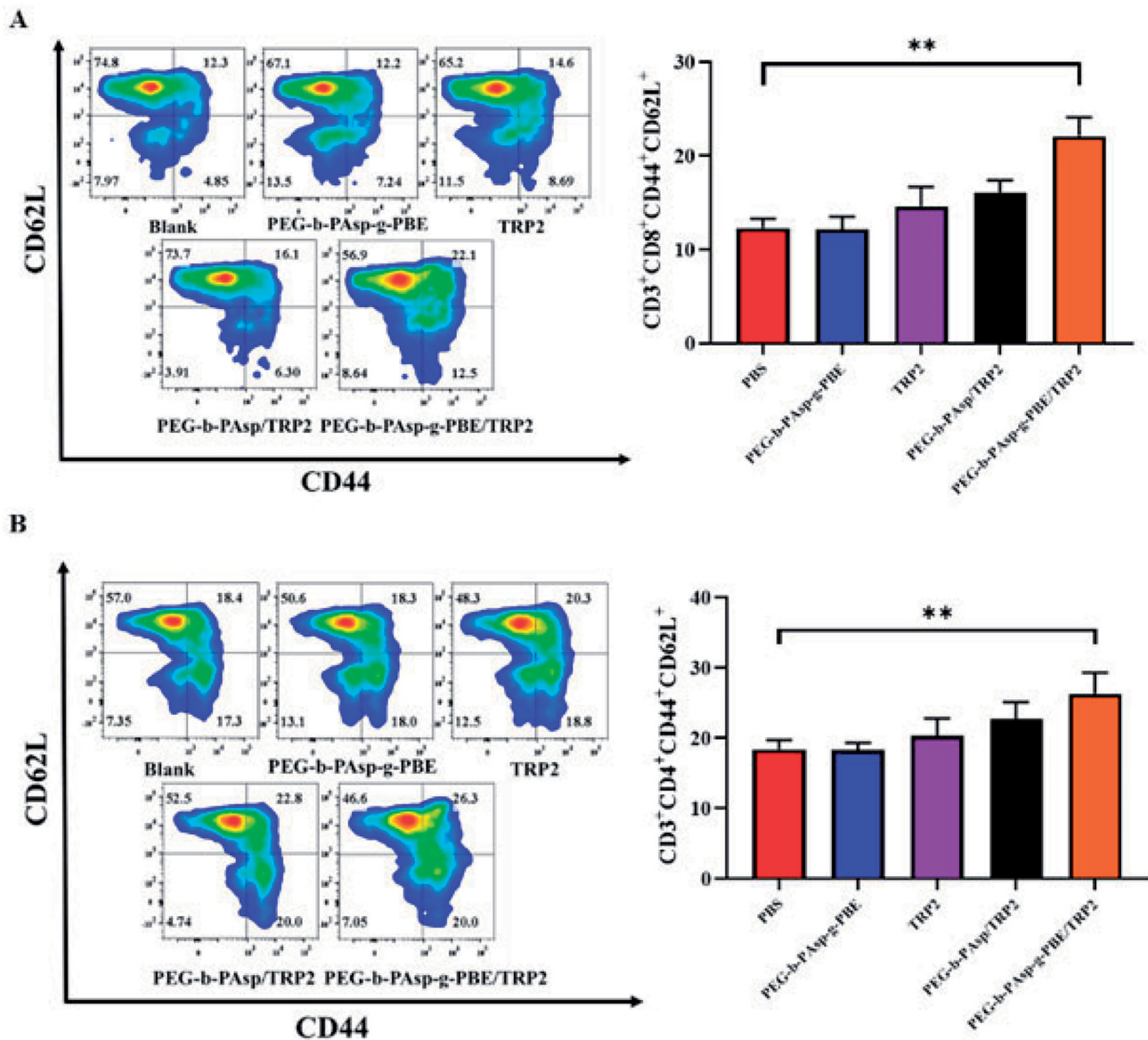


Figure 9. The representative flow cytometry images and statistic data of memory T-cell analysis (A) CD8⁺ and (B) CD4⁺ TCM by flow cytometry after re-stimulating with TRP2 (50 µg/mL) for 7 days after immunization. Results are presented as mean (SD) ($n = 5$) (** $P < .01$).

measured every 2 or 3 days (Figure 10(A)). No inhibitory effect on tumor growth was observed within the negative control groups (PBS, PEG-b-PAsp-g-PBE), and the average tumor volumes were 2452.09 mm³. However, all groups vaccination with (TRP2, PEG-b-PAsp/TRP2 and PEG-b-PAsp-g-PBE/TRP2) showed different levels of tumor growth inhibition effect. Especially, the group immunization with PEG-b-PAsp-g-PBE/TRP2 achieve significant delay in the tumor growth (complete elimination of tumors in ~78% of animals), compared to the other groups, including the TRP2 and PEG-b-PAsp/TRP2 groups (Figure 10(B,C)). All mice were sacrificed for immunity evaluation at day 21 days, splenocytes collected. Compared to positive group (TRP2, PEG-b-PAsp/TRP2), PEG-b-PAsp/TRP2 treatment could obviously improve the percentage of CD8⁺ T cells in splenocytes (Figure 10(D)). The enhanced tumor prevention effect identified PEG-b-PAsp/TRP2 nanovaccine can protect mice from challenged B16F10 melanoma cells.

Additionally, toxicity is a major concern for in vivo application of nanoparticles. The mice in each group showed obviously decreasing body weight (Figure 10(E)), indicating that negligible toxicity occurred during treatment. To further confirm, we sacrificed mice, collected all the organ tissues and preform the histological analysis at the end of experiment (Figure 10(F)). Compared with tissues of blank group, no obvious abnormality was found in each group. Collectively, these results demonstrate the vaccine delivery system with good biocompatibility suggest the potency in tumor prevention.

3.6. Antitumor efficacy study

Encouraged by above results, the therapeutic effect of nanovaccine was performed on the B16F10 melanoma model. Consistent with in vivo prophylactic effect data, PEG-b-PAsp-g-PBE/TRP2 nanovaccine exhibited robust antitumor efficacy,

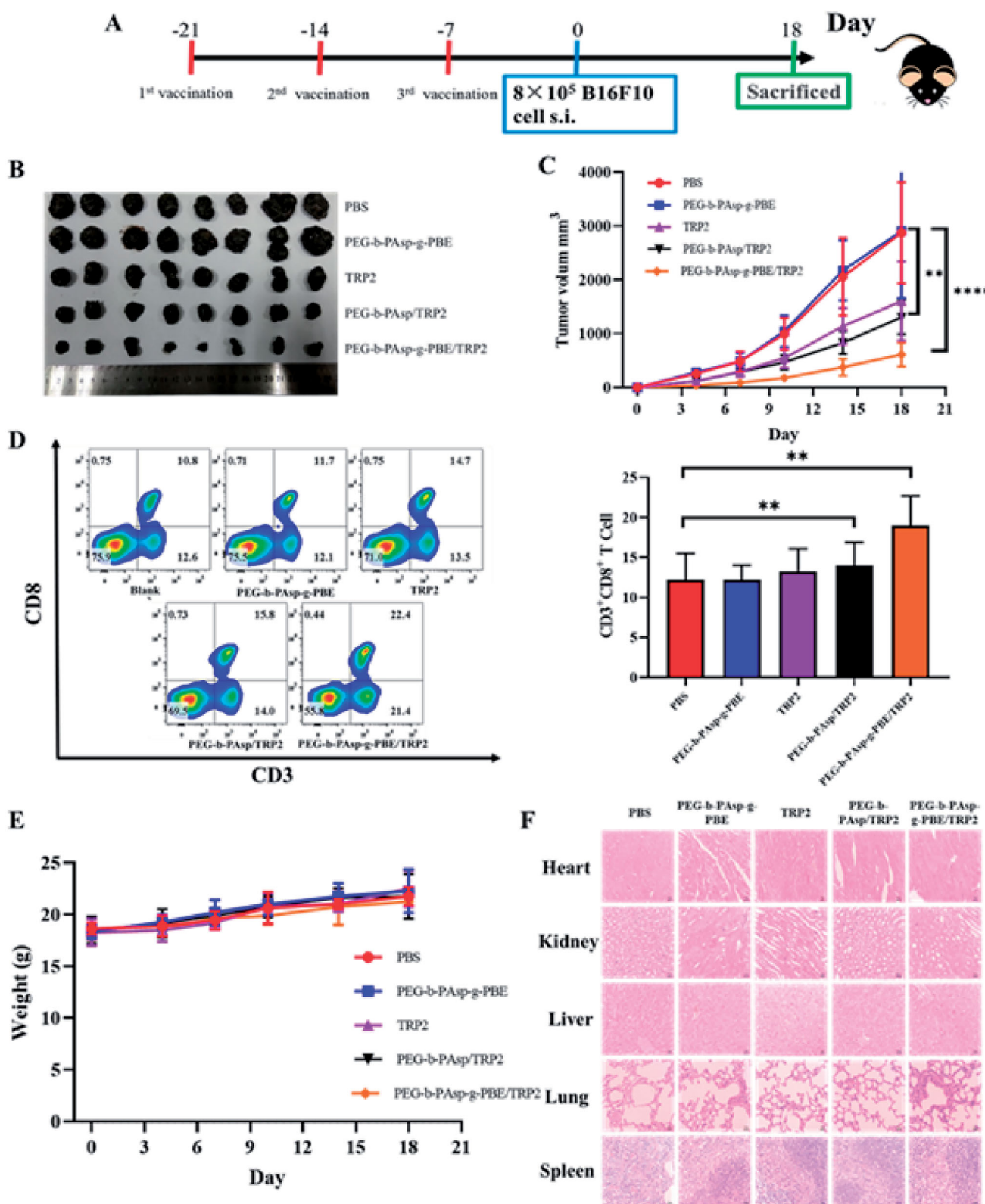


Figure 10. Antitumor effect of PEG-b-PAsp-g-PBE/TRP2 as a prophylactic vaccine (A) Schematic illustration for immune processes and tumor challenge experiment design. (B, C) Prophylactic effects of nanovaccine against B16F10 melanoma cells (B) Photo of tumor tissues from mice at the end of the study (C) Average tumor growth curves. (D) The representative flow cytometry images and statistic data of CD8⁺ T cells in the spleen from mice at the end of the study. (E) Real-time weight analysis of mice after each treatment. (F) Histological analysis of tissues with H&E Results are presented as mean (SD) (*n* = 8) (***P* < .01 and *****P* < .0001).

leading significant effects to suppress tumor growth. The tumor growth inhibition of the group PEG-b-PAsp-g-PBE/TRP2 injected with was 80.0% on the 18th day, while positive

group treated with TRP2 and PEG-b-PAsp/TRP2 were 26.3% and 66.3% respectively. TRP2 peptide only achieve limited antitumor and therapeutic effects without nanocarrier due to

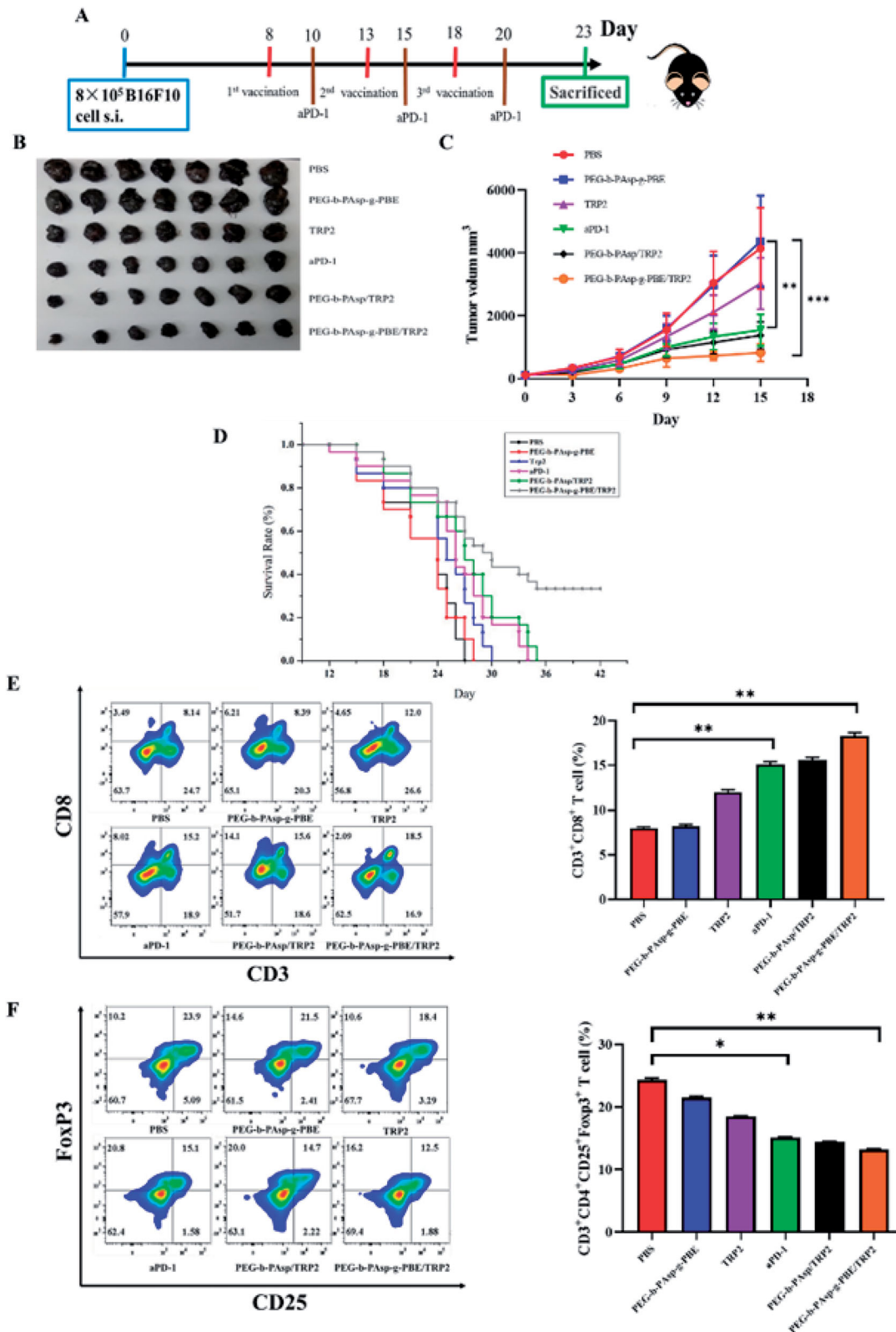


Figure 11. Antitumor effect of PEG-b-PAsp-g-PBE/TRP2 vaccine (A) Schematic illustration for immune processes and tumor challenge experiment design. (B, C) Antitumor effects of nanovaccine against B16F10 melanoma cells ($n = 7$) (B) Photo of tumor tissues from mice at the end of the study (C) average tumor growth curves. (D) Survival data of mice shown in panel ($n = 15$) (E) The representative flow cytometry images and statistic data of CD8⁺ T cells in the spleen from mice at the end of the study ($n = 7$). (F) The representative flow cytometry images and statistic data of Treg cells in the spleen from mice at the end of the study ($n = 7$). Results are presented as mean (SD) (* $P < .05$, ** $P < .01$ and *** $P < .001$).

its announced problem including rapid degradation, low affinity and immunological tolerance. Anti-PD-1, as one of immune checkpoint block (ICB), revitalize the cancer

immunotherapy and enhance the antitumor effect in clinic treatment for advanced melanoma. aPD-1 treated group showed moderate significantly retarded tumor growth (62%

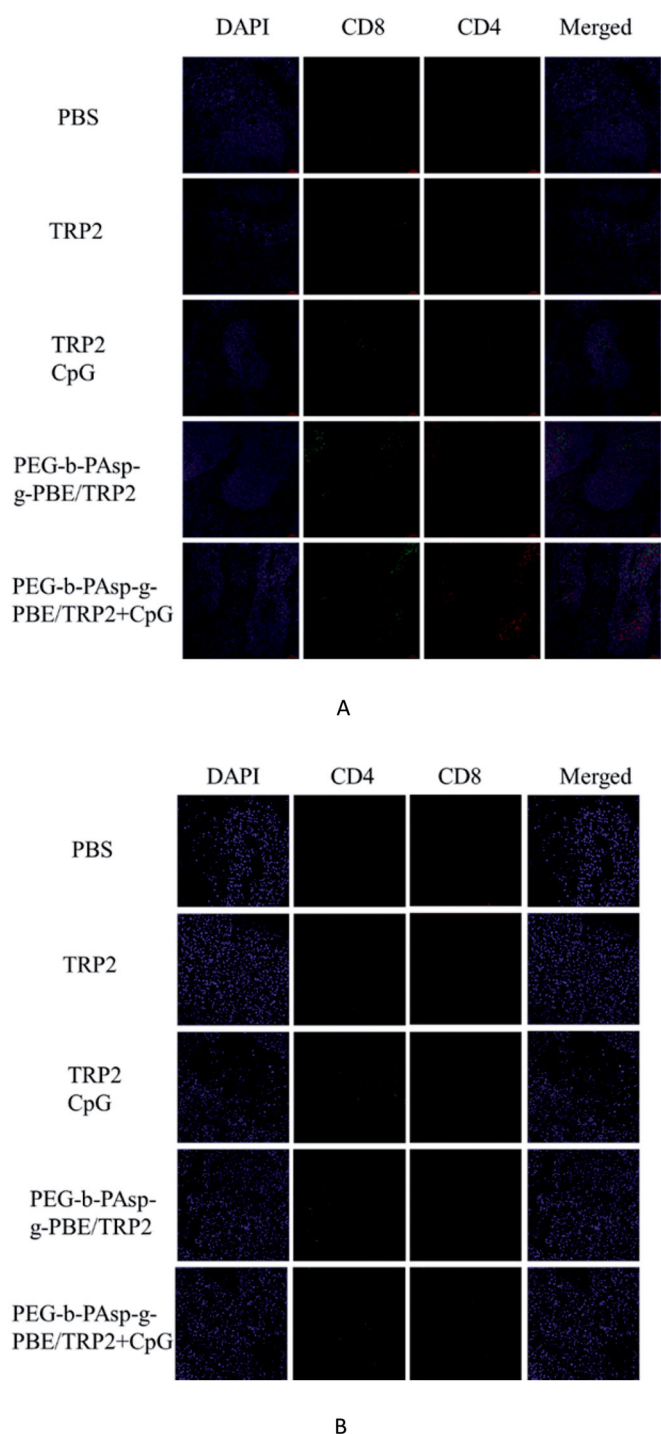


Figure 12. Immunofluorescence staining of splenocyte (A) and tumors (B) showed the CD8⁺ T cells, CD4⁺ T cells.

tumor growth inhibition), which was higher than TRP2-treated group (26.3%) and lower than PEG-b-PAsp-g-PBE/TRP2 group (80.0%) (Figure 11(B,C)).

Cytosine-phosphate-guanine (CpG) as the immunoadjuvants, has widely applied in the nanovaccine for promoting antigen-specific immune response through TLR 9 pathway. In order to further confirm the antitumor efficacy of this PEG-b-PAsp-g-PBE/TRP2 adjuvant-free nanovaccine, the combinations of CpG have been tested. As shown in Figure S14, the TRP2 + CpG group exhibit the more powerful tumor growth suppression

compared with the one treated with TRP2 only. However, compared with PEG-b-PAsp-g-PBE/TRP2 group, the addition of CpG (PEG-b-PAsp-g-PBE/TRP2 + CpG) showed only limited improvement in tumor inhibition. Therefore, the data further confirmed PEG-b-PAsp-g-PBE/TRP2 nanovaccine without external adjuvant did exhibit outstanding antitumor efficacy.

The survival rate of mice was recorded at the same time (Figure 11(D)). Noticeably, 40% of mice still survived 30 days after treated with PEG-b-PAsp-g-PBE/TRP2 nanovaccine and none of the mice survived in the two control groups (PBS and PEG-b-PAsp-g-PBE) after 27 days. PEG-b-PAsp-g-PBE/TRP2 adjuvant-free nanovaccine can facilitated a prolonged mean survival time and a significantly improved survival rate. Most strikingly, the PEG-b-PAsp-g-PBE/TRP2 group show longest survival time (nearly 33% of mice) after 36 days, while none of mice survived in other groups. Therefore PEG-b-PAsp-g-PBE/TRP2 adjuvant-free nanovaccine can not only show efficient anti-tumor activity but also prolong survival span of vaccinated mice in immunotherapy.

CD8⁺ T cell and CD4⁺CD25⁺FoxP3⁺ T cell (T regular cell) from splenocyte were analyzed by flow cytometry (Figure 11(E,F)). PEG-b-PAsp-g-PBE/TRP2 could obviously induced strong CTL response. The percentage of CD8⁺ T cells in splenocytes of this group is 18.5% which is 2.27-fold, 2.20-fold, 1.54-fold, 1.22-fold, 1.18-fold higher than PBS, PEG-b-PAsp-g-PBE, aPD-1, TRP2, PEG-b-PAsp/TRP2. Conversely Treg cell play a critical role in the immune response by down-regulating the function of effector T cell. The decrease in percentage of Treg cell was also reflected in the remarkable increase in effector T cell ratios. As shown the percentage of CD25⁺FoxP3⁺ Tregs decreased after treated with PEG-b-PAsp-g-PBE/TRP2 nanovaccine.

Toxicity evaluation also performed during the antitumor efficacy study in combination immunotherapy. Consistent with the prophylactic experiment, the results indicate the favorable biocompatibility of nanovaccine through body weights measurement and H&E stain (Figure S15 and S16).

Finally, the T cell from splenocyte and tumor sections were evaluated by immunofluorescence staining. As shown Figure 12 and Figure S17 and S18, TRP2 nanovaccine increased CD8⁺ T cell and also led to a decrease in immunosuppressive cell (Treg Cell). Also in tumor section, immunofluorescence signal of PD-1 is rather low in TRP2 nanovaccine treated group as compared with PBS group, further confirming the excellent ability of TRP2 nanovaccine to down-regulate immunosuppressive cell. Moreover, compared with the TRP2 nanovaccine, the addition of CpG (PEG-b-PAsp-g-PBE/TRP2 + CpG) did not showed apparent difference both in splenocyte and tumor sections. Taken together, these results suggested that the PEG-b-PAsp-g-PBE/TRP2 adjuvant-free nanovaccine induce a remarkable immune response and achieve immune prevention and protection.

4. Conclusions

In summary, we have developed the nanovaccine delivery system without any external adjuvant to overcome multiple limitation of peptide-based vaccine and boost immune

response in tumor prevention and treatment. According to principle of designing vaccine, we optimize PEG45-b-PAsp90 and PEG45-b-PAsp90-g-PBE50 as ideal polymers to fabricate nanovaccine, considering its cytotoxicity, size, charge, drug loading efficiency and cellular uptake. For PBE modification, PEG45-b-PAsp90-g-PBE50/TRP2 adjuvant-free nanovaccine can promote cellular uptake, stimulate DC maturation, enhance lymph node retention and improve T cell activation. Strikingly, PEG45-b-PAsp90-g-PBE50/TRP2 adjuvant-free nanovaccine elicited strong T-cell responses and led to potent tumor growth inhibition against melanoma both in prophylactic and therapeutic models. Furthermore, PEG45-b-PAsp90-g-PBE50/TRP2 can showed greater anti-tumor immune response than monotherapy treated with TRP2 peptide, with 33% survival over 36 days. Therefore, PEG-b-PAsp-g-PBE nanovaccine without any adjuvant can serve as an attractive candidate platform for effective antigen delivery in tumor immunotherapy due to its simplicity, safety and effectivity.

Author contributions

The manuscript was written through contributions of all authors.

Disclosure statement

No potential conflict of interest was reported by the authors.

Funding

The authors gratefully acknowledge the support of Natural Science Foundation of Jiangsu Province (Project BK20201333), 'Double First-Class' University project (CPU2018GY25) and Postgraduate Research & Practice Innovation Program of Jiangsu Province.

ORCID

Qiyang Wang  <http://orcid.org/0000-0001-6379-7879>

References

- Bu J, Nair A, Iida M, et al. (2020). An avidity-based PD-L1 antagonist using nanoparticle-antibody conjugates for enhanced immunotherapy. *Nano Lett* 20:4901–9.
- Chen Q, Chen G, Chen J, et al. (2019). Bioresponsive protein complex of aPD1 and aCD47 antibodies for enhanced immunotherapy. *Nano Lett* 19:4879–89.
- Chesson CB, Huelsmann EJ, Lacey AT, et al. (2014). Antigenic peptide nanofibers elicit adjuvant-free CD8⁺ cell responses. *Vaccine* 32: 1174–80.
- Dixit S, Sahu R, Verma R, et al. (2018). Caveolin-mediated endocytosis of the Chlamydia M278 outer membrane peptide encapsulated in poly(lactic acid)-Poly(ethylene glycol) nanoparticles by mouse primary dendritic cells enhances specific immune effectors mediated by MHC class II and CD4⁺ T cells. *Biomaterials* 159:130–45.
- Dong X, Liang J, Yang A, et al. (2019). A visible codelivery nanovaccine of antigen and adjuvant with self-carrier for cancer immunotherapy. *ACS Appl Mater Interfaces* 11:4876–88.
- Dong Z, Wang Q, Huo M, et al. (2019). Mannose-modified multi-walled carbon nanotubes as a delivery nanovector optimizing the antigen presentation of dendritic cells. *ChemistryOpen* 8:915–21.
- Gause KT, Wheatley AK, Cui J, et al. (2017). Immunological principles guiding the rational design of particles for vaccine delivery. *ACS Nano* 11:54–68.
- Guo YY, Wang D, Song QL, et al. (2015). Erythrocyte membrane-enveloped polymeric nanoparticles as nanovaccine for induction of antitumor immunity against melanoma. *ACS Nano* 9:6918–33.
- Hu Y, Lin L, Chen J, et al. (2020). Highly enhanced antitumor immunity by a three-barreled strategy of the l-arginine-promoted nanovaccine and gene-mediated PD-L1 blockade. *ACS Appl Mater Interfaces* 12: 41127–37.
- Hu Z, Ott PA, Wu CJ. (2018). Towards personalized, tumour-specific, therapeutic vaccines for cancer. *Nat Rev Immunol* 18:168–82.
- Hu X, Yu J, Qian C, et al. (2017). H2O2-responsive vesicles integrated with transcutaneous patches for glucose-mediated insulin delivery. *ACS Nano* 11:613–20.
- Irvine DJ, Hanson MC, Rakhra K, Tokatlian T. (2015). Synthetic nanoparticles for vaccines and immunotherapy. *Chem Rev* 115:11109–46.
- John TW, Salka K, Matthew JM, et al. (2013). *ACS Nano* 7:3912–25.
- Kakwere H, Ingham ES, Allen R, et al. (2017). Toward personalized peptide-based cancer nanovaccines: a facile and versatile synthetic approach. *Bioconjug Chem* 28:2756–71.
- Kapadia CH, Tian S, Perry JL, et al. (2016). Reduction sensitive PEG hydrogels for codelivery of antigen and adjuvant to induce potent CTLs. *Mol Pharm* 13:3381–94.
- Kuai R, Ochyl LJ, Bahjat KS, et al. (2017). Designer vaccine nanodiscs for personalized cancer immunotherapy. *Nat Mater* 16:489–96.
- Kuai R, Sun X, Yuan W, et al. (2018). Subcutaneous nanodisc vaccination with neoantigens for combination cancer immunotherapy. *Bioconjug Chem* 29:771–5.
- Lai C, Duan S, Ye F, et al. (2018). The enhanced antitumor-specific immune response with mannose- and CpG-ODN-coated liposomes delivering TRP2 peptide. *Theranostics* 8:1723–39.
- Li HM, Dong ZP, Wang QY, et al. (2017). De novo computational design for development of a peptide ligand oriented to VEGFR-3 with high affinity and long circulation. *Mol Pharm* 14:2236–44.
- Li X, Cai X, Zhang Z, et al. (2020). Mimetic heat shock protein mediated immune process to enhance cancer immunotherapy. *Nano Lett* 20: 4454–63.
- Liu L, Cao F, Liu X, et al. (2016). Hyaluronic acid-modified cationic lipid-PLGA hybrid nanoparticles as a nanovaccine induce robust humoral and cellular immune responses. *ACS Appl Mater Interfaces* 8: 11969–79.
- Liu Y, Yao L, Cao W, et al. (2019). Dendritic cell targeting peptide-based nanovaccines for enhanced cancer immunotherapy. *ACS Appl Bio Mater* 2:1241–54.
- LiuJiang ZW, Nam J, Moon JJ, et al. (2018). Immunomodulating nanomedicine for cancer therapy. *Nano Lett* 18:6655–9.
- Lu Y, Aimetti AA, Langer R, Gu Z. (2016). Bioresponsive materials. *Nat Rev Mater* 2.
- Mahasa KJ, Ouifki R, Eladdadi A, Pillis L. d. (2016). Mathematical model of tumor-immune surveillance. *J Theor Biol* 404:312–30.
- Malonis RJ, Lai JR, Vergnolle O. (2019). Peptide-based vaccines: current progress and future challenges. *Chem Rev* 120:3210–29.
- Manaster AJ, Batty C, Tiet P, et al. (2019). Oxidation-sensitive dextran-based polymer with improved processability through stable boronic ester groups. *ACS Appl Bio Mater* 2:3755–62.
- Martin JD, Cabral H, Stylianopoulos T, Jain RK. (2020). Improving cancer immunotherapy using nanomedicines: progress, opportunities and challenges. *Nat Rev Clin Oncol* 17:251–66.
- Melero I, Gaudernack G, Gerritsen W, et al. (2014). Therapeutic vaccines for cancer: an overview of clinical trials. *Nat Rev Clin Oncol* 11: 509–24.
- Merlo A, Dalla Santa S, Dolcetti R, et al. (2016). Reverse immunoediting: when immunity is edited by antigen. *Immunol Lett* 175:16–20.
- Mora-Solano C, Wen Y, Han H, et al. (2017). Active immunotherapy for TNF-mediated inflammation using self-assembled peptide nanofibers. *Biomaterials* 149:1–11.
- Musetti S, Huang L. (2018). Nanoparticle-mediated remodeling of the tumor microenvironment to enhance immunotherapy. *ACS Nano* 12: 11740–55.

- Naito M, Yoshinaga N, Ishii T, et al. (2017). Enhanced intracellular delivery of siRNA by controlling ATP-responsivity of phenylboronic acid-functionalized polyion complex micelles. *Macromol Biosci* 18:1700357.
- Paijens ST, Vledder A, de Bruyn M, Nijman HW. (2021). Tumor-infiltrating lymphocytes in the immunotherapy era. *Cell Mol Immunol* 18:842–59.
- Rajput MKS, Kesharwani SS, Kumar S, et al. (2018). Dendritic cell-targeted nanovaccine delivery system prepared with an immune-active polymer. *ACS Appl Mater Interfaces* 10:27589–602.
- Riley RS, June CH, Langer R, Mitchell MJ. (2019). Delivery technologies for cancer immunotherapy. *Nat Rev Drug Discov* 18:175–96.
- Sengupta N, MacFie TS, MacDonald TT, et al. (2010). Cancer immunoeediting and "spontaneous" tumor regression. *Pathol Res Pract* 206:1–8.
- Shae D, Baljon JJ, Wehbe M, et al. (2020). Co-delivery of peptide neoantigens and stimulator of interferon genes agonists enhances response to cancer vaccines. *ACS Nano* 14:9904–16.
- Shi W, Tong Z, Qiu Q, et al. (2020). Novel HLA-A2 restricted antigenic peptide derivatives with high affinity for the treatment of breast cancer expressing NY-ESO-1. *Bioorg Chem* 103:104138.
- Singha S, Shao K, Ellestad KK, et al. (2018). Nanoparticles for immune stimulation against infection, cancer, and autoimmunity. *ACS Nano* 12:10621–35.
- Slingluff CL. (2011). The present and future of peptide vaccines for cancer: single or multiple, long or short, alone or in combination? *Cancer J* 17:343–50.
- Sun Q, Bai X, Sofias AM, et al. (2020). Cancer nanomedicine meets immunotherapy: opportunities and challenges. *Acta Pharmacol Sin* 41:954–8.
- Ugur S, Özlem T. (2018). Tumor-infiltrating lymphocytes in the immunotherapy era. *Cancer Immunother* 359:1355–60.
- Varade J, Magadan S, Gonzalez-Fernandez A. (2021). Human immunology and immunotherapy: main achievements and challenge. *Cell Mol Immunol* 18:805–28.
- Vrbata D, Uchman M. (2018). Preparation of lactic acid- and glucose-responsive poly(ϵ -caprolactone)-*b*-poly(ethylene oxide) block copolymer micelles using phenylboronic ester as a sensitive block linkage. *Nanoscale* 10:8428–42.
- Wang J, Mamuti M, Wang H. (2020). Therapeutic vaccines for cancer immunotherapy. *ACS Biomater Sci Eng* 6:6036–52.
- Wang K, Wen S, He L, et al. (2018). "Minimalist" nanovaccine constituted from near whole antigen for cancer immunotherapy. *ACS Nano* 12:6398–409.
- Wang QY, Li HM, Dong ZP, et al. (2019). Peptide-mediated cationic micelles drug-delivery system applied on a VEGFR3-overexpressed tumor. *J Mater Chem B* 7:1076–86.
- Wang QY, Xu YS, Zhang NX, et al. (2020). Phenylboronic ester-modified anionic micelles for ROS-stimuli response in HeLa cell. *Drug Deliv* 27:681–90.
- Wiedermann U, Davis AB, Zielinski CC. (2013). Vaccination for the prevention and treatment of breast cancer with special focus on Her-2/neu peptide vaccines. *Breast Cancer Res Treat* 138:1–12.
- Wu X, Li Y, Chen X, et al. (2019). A surface charge dependent enhanced Th1 antigen-specific immune response in lymph nodes by transferosome-based nanovaccine-loaded dissolving microneedle-assisted transdermal immunization. *J Mater Chem B* 7:4854–66.
- Xu Q, He C, Xiao C, Chen X. (2016). Reactive oxygen species (ROS) responsive polymers for biomedical applications. *Macromol Biosci* 16:635–46.
- Yang F, Shi K, Jia Y-p, et al. (2020). Advanced biomaterials for cancer immunotherapy. *Acta Pharmacol Sin* 41:911–27.
- Yang H, Zhang C, Li C, et al. (2015). Glucose-responsive polymer vesicles templated by α -CD/PEG inclusion complex. *Biomacromolecules* 16:1372–81.
- Zeng Q, Gammon JM, Tostanoski LH, et al. (2017). In vivo expansion of melanoma-specific T cells using microneedle arrays coated with immune-polyelectrolyte multilayers. *ACS Biomater Sci Eng* 3:195–205.
- Zhang L, Wu S, Qin Y, et al. (2019). Targeted Codelivery of an antigen and dual agonists by hybrid nanoparticles for enhanced cancer immunotherapy. *Nano Lett* 19:4237–49.
- Zhang M, Hong Y, Chen W, Wang C. (2017). Polymers for DNA vaccine delivery. *ACS Biomater Sci Eng* 3:108–25.
- Zhang Y, Zhang Z. (2020). The history and advances in cancer immunotherapy: understanding the characteristics of tumor-infiltrating immune cells and their therapeutic implications. *Cell Mol Immunol* 17:807–21.
- Zhao H, Xu J, Li Y, et al. (2019). Nanoscale coordination polymer based nanovaccine for tumor immunotherapy. *ACS Nano* 13:13127–35.
- Zhao H, Zhao B, Wu L, et al. (2019). Amplified cancer immunotherapy of a surface-engineered antigenic microparticle vaccine by synergistically modulating tumor microenvironment. *ACS Nano* 13:12553–66.
- Zhu G, Zhang F, Ni Q, et al. (2017). Efficient nanovaccine delivery in cancer immunotherapy. *ACS Nano* 11:2387–92.
- Zupancic E, Curato C, Kim JS, et al. (2018). Nanoparticulate vaccine inhibits tumor growth via improved T cell recruitment into melanoma and huHER2 breast cancer. *Nanomedicine* 14:835–47.